Fungal Biology 129 (2025) 101668

Contents lists available at ScienceDirect

Fungal Biology

journal homepage: www.elsevier.com/locate/funbio

Effector molecules and pathogenicity-associated gene expression in *Ascochyta rabiei*

Mahmuda Binte Monsur *, Ido Bar, Jonathan Wanderley Lawley, Rebecca Ford

School of Environment and Science, Griffith University, QLD, 4111, Australia

ARTICLE INFO

Keywords:
Ascochyta rabiei
Pathogenicity
Effector molecules
Transcriptomics
Dual RNA-seq

ABSTRACT

The necrotrophic fungus *Ascochyta rabiei* poses a significant threat to chickpea cultivation worldwide, leading to severe yield losses and quality reduction. Understanding the molecular mechanisms behind the pathogenicity of *A. rabiei* is essential for developing effective management strategies. This study employed transcriptomic analyses to compare the gene expression profiles among two *A. rabiei* isolates with differing pathogenicity levels (highly pathogenic AR0231 and low pathogenic AR0225) during interaction of PBA HatTrick chickpea genotype at the early podding stage. PBA HatTrick is classified as moderately susceptible to *A. rabiei* based on field trial ratings from the GRDC National Variety Trials. Like most cultivated chickpea varieties, its resistance to *A. rabiei* is generally considered polygenic and quantitative in nature, with no major resistance gene identified to date. A total of 105 differentially expressed genes (DEGs) were identified, including 57 upregulated and 48 downregulated in AR0231. Notably, effector-related genes were prominent among the upregulated DEGs, including EKO05_0002468, a homolog of the CoNIS1 effector gene that suppresses plant immunity, and EKO05_0010552, a homolog of PsGIP2/PsGIP1 encoding a glucanase inhibitor that protects fungal cell walls from host enzymes. Additionally, EKO05_0001368, homologous to PesCDA/VdPDA1, encodes a chitin-binding effector linked to immune evasion. Downregulated DEGs included EKO05_0006947, a LysM-domain effector homolog implicated in masking fungal chitin from host detection. These findings provide new insights into the molecular mechanisms employed by *A. rabiei* during infection of mature chickpea tissue and highlight candidate genes for future research on improving chickpea resistance to Ascochyta blight.

1. Introduction

Ascochyta blight, caused by the necrotrophic filamentous fungus *Ascochyta rabiei*, poses a significant challenge to worldwide chickpea cultivation (Pande et al., 2005; Singh and Reddy, 1993; Trapero-Casas and Kaiser, 1992). Symptoms develop on all aerial parts of the plant but are most prominent during the flowering to early podding stages when they cause interference with normal photosynthesis and growth, leading to seed shriveling, discoloring and abortion (Pande et al., 2005; Sharma and Ghosh, 2016). Under favourable conditions and without appropriate disease management practices, such as the use of tolerant chickpea varieties and preventative fungicide applications, the disease can cause severe quality reduction and up to 100 % yield loss (Nene et al., 2012; Nene, 2008). In Australia alone, the average annual loss is AUD 4.8 million (Foresto et al., 2023; Newman et al., 2021), with the management of *A. rabiei* becoming ever more challenging due to the emergence of highly pathogenic pathotypes at increasing rates (Bar et al., 2021; Bretag et al., 2008). The rapid evolution of these pathotypes is likely driven by host-imposed selection pressures (Singh et al., 2022). Recent whole-genome sequencing studies have identified specific SNP loci associated with aggressiveness in *A. rabiei* populations (Vaghefi et al., 2024), although the functional relevance of these loci remains largely unknown.

Effector molecules are central to the pathogenicity of necrotrophic fungi (Brown and Kosack, 2015; Li et al., 2022). In *A. rabiei*, several candidate effectors have been identified through transcriptomic profiling, including those encoding small secreted proteins (SSPs) and other genes differentially expressed during infection (Fondevilla et al., 2015; Verma et al., 2017). A recent study functionally characterized ArPEC25, a nuclear-localized effector that targets the chickpea transcription factor CaβLIM1a to suppress lignin biosynthesis, weakening cell wall defenses and enhancing susceptibility (Singh et al., 2023). These findings demonstrated that effector activity can extend beyond immunity suppression to structural manipulation of host tissues.

* Corresponding author.
E-mail address: mahmudabinte.monsur@griffithuni.edu.au (M.B. Monsur).

https://doi.org/10.1016/j.funbio.2025.101668
Received 19 April 2025; Received in revised form 30 September 2025; Accepted 4 October 2025
Available online 5 October 2025

However, the majority of *A. rabiei* effectors remain uncharacterized, and their contributions to virulence, host specificity, and immune evasion are not yet fully understood. The recent targeted mutation of the succinate dehydrogenase subunit B has enabled more efficient transformation and functional validation of effector candidates in *A. rabiei* (Debler et al., 2025).

Several effector classes with defined immunity-suppressive roles have been described in other fungal pathosystems but are yet to be functionally validated in *A. rabiei*. For example, *Verticillium dahliae* produces a chitin deacetylase (VdPDA1) that alters fungal cell wall components to avoid recognition by host immune receptors (Volk et al., 2019), while *Cladosporium fulvum* secretes LysM-domain effectors that bind chitin fragments and prevents their detection by host pattern recognition receptors (Jonge et al., 2010; Jonge and Thomma, 2009). Although *A. rabiei* encodes homologs of these effector types, their roles in immune evasion remain speculative.

Most functional studies in *A. rabiei* to date have focused on seedling or early vegetative stages of chickpea (Basandrai et al., 2007; Sharma and Pande, 2010), leaving later developmental stages underexplored. The early podding stage is particularly important, as this is when the plant prioritizes resource allocation toward seed filling and reproductive success. During this phase, defense responses such as reactive oxygen species (ROS) production, pathogenesis-related (PR) gene expression, and salicylic acid-mediated signaling are downregulated or delayed (Chongo et al., 2001), making the host more vulnerable to infection. Severe disease at this stage can result in reduced marketable yield due to pod lesions or complete yield loss due to the plant's reduced capacity for recovery.

To uncover a deeper understanding of *A. rabiei* effectors and other pathogenicity associated molecules, this study uses RNA sequencing to: (1) identify differentially expressed genes (DEGs) between two *A. rabiei* isolates with contrasting pathogenicity during early podding-stage infection of chickpea, (2) examine candidate genes involved in immune evasion, nutrient uptake, and metabolic adaptation, and (3) highlight effector molecules that contribute to host recognition and invasion.

2. Materials and methods

2.1. A. rabiei isolates and plant material

Two *A. rabiei* isolates from the Griffith University *A. rabiei* collection that demonstrate distinct low and high pathogenicity across a differential host set (AR0225 and AR0231) were chosen for this study (Bar et al., 2021; Sambasivam et al., 2020a). The isolate pathogenicity metadata is available on the publicly accessible Ascochyta Dashboard (https://shinotate.pp18000.cloud.edu.au/shiny/Asco_dashboard/). According to the Dashboard and prior lesion scoring data, AR0231 was consistently classified as belonging to pathogenicity group (PG) 5, indicative of high aggressiveness and severe disease expression, while AR0225 was categorized as a PG 1 isolate, indicating low aggressiveness and minimal lesion development. The chosen isolates originate from the highly clonal Australian *A. rabiei* population, with a highly similar genetic background, based on whole genome single nucleotide polymorphism diversity analysis (Vaghefi et al., 2024). The low pathogenic isolate AR0225 was collected in 2020 from chickpea cv. PBA Seamer grown in Narromine, New South Wales, Australia and the high pathogenic isolate AR0231 was collected in 2020 from cv. PBA HatTrick grown in Narwonah, New South Wales, Australia.

Isolate cultures were established by transferring water-stored mycelial agar plugs onto fresh V8 juice agar plates (90 mm Petri dish with 20 ml V8 juice agar). Plates were then sealed with parafilm M® and incubated at 20 ± 2 °C for 14 days. To expose the isolates to the mature host tissues, plants of the moderately susceptible PBA HatTrick chickpea cultivar were grown in a controlled-environment growth room at 26 °C ± 2 °C under a 12-h light/12-h dark cycle. Three biological replicates, each consisting of three plants per pot (135 × 140 mm), were cultivated in Searles advanced potting mix soil and maintained for approximately 10 weeks until the early podding stage. Plants were sprayed until run-off with a 1×10^5 conidiospore suspension of *A. rabiei* AR0225 or AR0231 isolate. The spore suspension was prepared in sterile water with the addition of 2–3 drops of Tween 20 per 100 mL (equivalent to 0.02 % v/v) to act as a surfactant and ensure even leaf coverage. Water containing Tween 20 was used as a negative control (Christie et al., 2021). Leaf samples were collected from each pot (replicate) at 12 and 72 h post inoculation (hpi). Based on prior studies, 12 hpi corresponds to the spore germination and early penetration phase, while 72 hpi reflects the onset of intracellular colonization prior to visible lesion development (Sambasivam et al., 2020b). Samples were instantly frozen in liquid N_2 and stored at −80 °C until RNA extraction (Fig. 1). Development of disease symptoms (leaf, pod and stem lesions) was observed visually approximately three weeks post-inoculation in inoculated plants to confirm establishment of the disease and differential disease response between the isolates.

2.2. RNA extraction and cDNA synthesis

Leaf samples (100 mg) were pulverized while frozen in liquid N_2 using a TissueLyser at 30 Hz for 30 s × 4 times. Samples were homogenized in 2 mL centrifuge tubes, each containing three stainless steel beads (2.4 mm diameter). The samples were kept frozen during homogenization by resubmerging them in liquid nitrogen for 30s between each homogenizing cycle. Total RNA was extracted using the NucleoZOL (Macherey–Nagel) following the manufacturer's protocol and were treated with DNase to using the TURBO DNA-free™ Kit (Invitrogen). The RNA concentration, purity and integrity were assessed using Nanodrop (Thermo-Fisher Scientific), Qubit 3 (Invitrogen) and gel electrophoresis (2 % agarose gel), respectively.

cDNA synthesis was performed using the SensiFAST™ cDNA Synthesis Kit (Bioline) following the manufacturer's instructions. A total of 1 μg RNA was used as a template for reverse transcription in a reaction volume of 20 μL. The synthesized cDNA was then used for downstream qPCR analysis.

2.3. RNA sequencing and transcript quantification

A quantity of 2 μg of each high-quality RNA was sequenced using the Illumina NovaSeq platform (S2 flow cell) by the Australian Genome Research Facility (AGRF; Melbourne, Victoria). Subsequently, the Illumina bcl2fastq 2.20.0.422 pipeline facilitated the conversion of base calls to fastq format for sequence data generation. Raw sequencing reads were obtained from AGRF and uploaded into the Galaxy Australia web platform (http://usegalaxy.org.au) for further processing (Afgan et al., 2018). A custom workflow was developed to identify transcripts and obtain read counts (Fig. 1). First, adaptor trimming and low-quality bases/reads removal was performed with fastp v0.23.2 with default parameters (Chen et al., 2018). Trimmed reads were then mapped to the *A. rabiei* reference genome, strain Me14 (NCBI accession GCA_004011695.2 (Shah et al., 2020); using bwa-mem 2 v2.2.2.1 with default parameters (Vasimuddin et al., 2019). This was followed by the specification of read groups for each sample, marking duplicates, and conversion of the alignments into coordinate-sorted indexed BAM files using Picard v2.18.2 (https://broadinstitute.github.io/picard/). Read counts were assigned to gene features using featureCounts v1.6.4 based on the Me14 reference genome annotation. Mapping statistics were obtained with Qualimap v2.2.2 d (Liao et al., 2013) and combined with trimming and read assignment statistics into a single interactive report using MultiQC v1.11 (Ewels et al., 2016; Okonechnikov et al., 2016).

2.4. Differential gene expression analysis

Differential gene expression analyses were performed on the

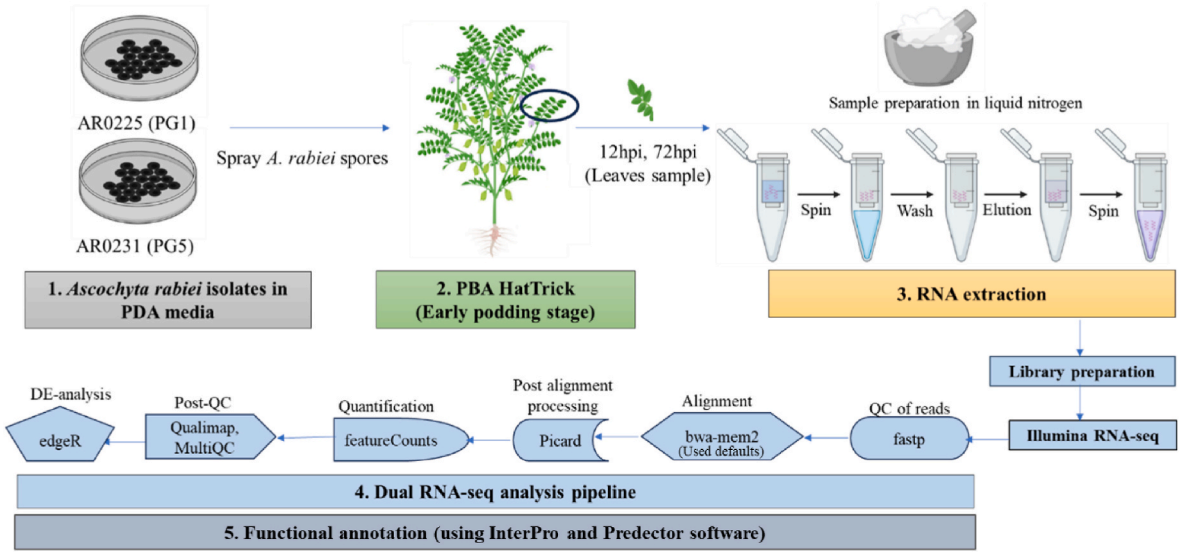

Fig. 1. Experimental design and RNA-Seq bioinformatics analysis pipeline of *A. rabiei* infecting chickpea.

featureCounts output count matrix using edgeR v3.26.8 in the R v3.6.1 language and environment for statistical computing (Y. Chen et al., 2014). Prior to analysis, the Trimmed Mean of M-values (TMM) normalization method was applied to the raw count data to account for differences in library sizes and reduce technical biases between samples. This method adjusted the gene expression levels to make them comparable across samples, ensuring accurate identification of differentially-expressed genes (DEG)s. Computed p-values were adjusted using the Benjamin–Hochberg false discovery rate (FDR) correction to account for multiple comparisons with an absolute $\log_2$ of the fold change ($|\log_2 FC|$) >1.5 and an FDR <0.05 as criteria used to determine differential expression. The edgeR package was used for data normalization and log-CPM calculation, while ggplot 2 v3.5.1 package was used to visualize the outputs (Wickham, 2009).

2.5. Quantitative real-time PCR (qPCR) analysis

To validate the transcriptomic differential gene expression results, four differentially expressed genes (FGL1, GIP1, PDA1, and Six 3) were selected for qPCR analysis. For this, 1 μg of the same RNA samples used for RNA-Seq was converted to cDNA using the SensiFAST™ cDNA Synthesis Kit (Bioline), and this cDNA was used as the template for qPCR. Each sample included three biological replicates and three technical replicates. Primers for all genes were designed using Primer 3 software (Supplementary Table 1), ensuring specificity to the *A. rabiei* genome reference (NCBI ID: GCF_004011695.2). Primer efficiencies were determined using a five-point, 10-fold serial dilution standard curve, starting from an initial cDNA concentration of 100 ng/μL, with serial dilutions of 100, 10, 1, 0.1, and 0.01 ng/μL. The reaction efficiency was estimated from the slope of the standard curve, and values were expressed as Eff values, calculated using the formula: $\text{Eff} = 10^{-1/\text{slope}}$. Eff values indicate the relative amplification performance of each primer set, where an Eff value of 2.00 corresponds to perfect doubling of DNA per cycle. The obtained Eff values for each gene and R^2 values are provided in supplementary data (Supplementary Table 1). qPCR reactions were carried out in 10 μL reaction volumes using SYBR Green Master Mix (Thermo Fisher Scientific) in a CFX96 Real-Time PCR Detection System (Bio-Rad). The thermal cycling conditions were 95 °C for 2 min, 40 cycles of 95 °C for 10 s and 60 °C for 30 s.

The reference genes EF1-α (EKO05_0003491) and PEP1 (EKO05_0002228) were used to normalize for variations in input cDNA across samples, ensuring accurate quantification of target gene expression levels. These genes were selected based on its stable expression in related species (Che et al., 2016), and their expression levels were examined in transcriptomic dataset, where both genes exhibited consistent expression across the two *A. rabiei* isolates. A pooled cDNA sample was prepared by combining equal aliquots from two experimental samples. It was included on each qPCR plate to serve as an inter-plate calibrator to ensure consistency across runs. The ΔΔCq method was applied to determine relative gene expression (Pfaffl, 2001). qRAT software was used to process raw Cq values, normalize expression based on reference genes (Flatschacher et al., 2022). Statistical significance of differential expression was assessed using the Kruskal–Wallis non-parametric test on ΔΔCq values ($p < 0.05$) (Kruskal and Wallis, 1952; Qi et al., 2014). Final bar graph with error bars was generated in Microsoft Excel, with fold change values plotted as mean ± standard error. The error bars indicate the standard error of the mean, calculated from biological replicates.

2.6. Effector prediction, annotation and domain analysis

Effectors were predicted using the effector prediction tool Predector v1.2.7, which integrates features such as signal peptides, transmembrane domains, and effector-like properties (Jones et al., 2021). The higher the effector score, the greater the probability that the DEG functions as a true effector. In this study, DEGs with positive Predector scores were considered putative effectors (e.g., GIP1, PDA1) and novel candidate effectors not previously annotated in the Me14 genome or CCDM datasets (e.g., EKO05_0002468, EKO05_0010011). Functional domains of these genes were assessed using InterProScan v5.66–98.0 to further classify their potential roles in pathogenicity.

3. Results

3.1. RNA sequencing and data quality control

RNA-Sequencing generated 214.2 ± 35.5 million reads per sample, with approximately 5 % of the reads mapped to the *A. rabiei* genome (see Supplementary Table 2 for details). To ensure data quality and minimize technical biases, the Trimmed Mean of M-values (TMM) normalization method was applied to the raw count data. This normalization accounted for differences in sequencing depth and RNA composition between libraries, which can introduce systematic bias in expression estimates. The count data was transformed and represented as log-transformed counts per million reads (log-CPM) to visualize the distribution of each library before and after normalization (A and B, respectively in

Supplementary Fig. 1). Prior to normalization, expression distributions varied substantially across samples due to differences in total read depth, gene composition, and RNA yield during library preparation. After TMM normalization, the expression distributions became more consistent across samples, as indicated by the aligned medians and reduced variability.

3.2. Gene expression analysis

When assessing for visual patterns of relationships among the DEGs, the largest two eigenvalues in the PCA plot accounted for 18.8 % and 12 % of the total variance, respectively (Fig. 2).

The PCA plot indicates that gene expression differences are primarily influenced by the genetic background of the isolates, which also differ in pathogenicity. While this suggests a link between pathogenicity and gene expression, the relatively low variance explained by principal components 1 and 2 (30.8 %) implies that additional biological or technical factors may also influence the gene expression patterns. Notably, there wasn't a clear separation between the two sampling time points (12 hpi vs. 72 hpi), indicating that the time of infection is not the primary driver of gene expression differences in this dataset.

To further explore the differences in gene expression, a heatmap of the top 1000 DEGs was generated (Supplementary Fig. 2). As sampling time had minimal impact on gene expression compared to the strong influence of isolate pathogenicity, we combined the 12 hpi and 72 hpi samples for subsequent analyses, focusing on identifying DEGs linked to the pathogenicity levels of the isolates. Additionally, one sample, labelled '31-L11,' was identified as an outlier, showing a distinct expression pattern that separated it from the main cluster. This outlier was excluded from further DEG analysis to maintain the robustness of our results.

A total of 105 differentially expressed genes (48 upregulated and 57 downregulated) were identified when comparing AR0231 (highly pathogenic) to AR0225 (less pathogenic), using AR0225 as the reference. The analysis applied a significance threshold of FDR <0.05 and an absolute log 2 fold change ($|\log2FC| > 1.5$ (Supplementary Fig. 3).

3.2.1. Host interaction and immune evasion

A set of genes associated with host interaction and immune evasion were found to be upregulated in the highly pathogenic isolate. The EKO05_0002468 gene, classified as a hypothetical protein due to the absence of functional annotation in BLAST and InterPro searches, was identified as effector using Predector (effector score: 0.45). Predector analysis linked this gene to NIS1 effectors (CoNIS1/MoNIS1/ChNIS1), which are known for their roles in host penetration and nutrient uptake (Table 1). The gene exhibited the highest upregulation in AR0231 ($Log_2FC = 8.12$), supporting its likely involvement in pathogenicity and immune evasion. Following this, EKO05_0000089 ($Log_2FC = 6.04$) matched FGL1/RsAGLIP1, an effector linked to the pathogen's virulence by enhancing its ability to manage oxidative stress within host tissues. EKO05_0003549 ($Log_2FC = 5.39$), an uncharacterized protein with an effector score of 0.58, was identified in AR0231. Its upregulation in this isolate implies a role in immunity suppression or other pathogenicity-related processes, although further functional characterization is needed. Similarly, the gene EKO05_0010552, identified *as PsGIP2/PsGIP1* ($Log_2FC = 5.35$), was significantly upregulated in AR0231. This glucanase inhibitor protein is known to inhibit host enzymes targeting fungal cell walls, thus helping evade host defenses. This mechanism of immune evasion aligns with the effector score of 0.96 associated with this protein. Another uncharacterized gene, EKO05_0010011, showed substantial upregulation in AR0231 ($Log_2FC = 5.33$) with a high effector score of 0.92. EKO05_0003368, encoding 2-Aminomuconic semi-aldehyde dehydrogenase, was upregulated in AR0231 ($Log_2FC = 2.35$). Similarly, EKO05_0001368, encoding a chitin-binding protein, was also upregulated in AR0231 ($Log_2FC = 2.01$). This protein matches effectors like PesCDA/VdPDA1/VnaChtBP, known for chitin deacetylase activity, which converts chitin to chitosan, thereby evading host chitin-triggered immunity.

In contrast, several genes were downregulated in highly pathogenic AR0231. For example, EKO05_0006947, with a Log_2FC of -2.12, matched RsLysM/MoCDIP11, a LysM domain effector known to bind chitin and mask fungal presence from host immune detection. Additionally, EKO05_0006932 ($Log_2FC = -3.55$), recognized as FolSix3, involved in immune evasion (Table 1)

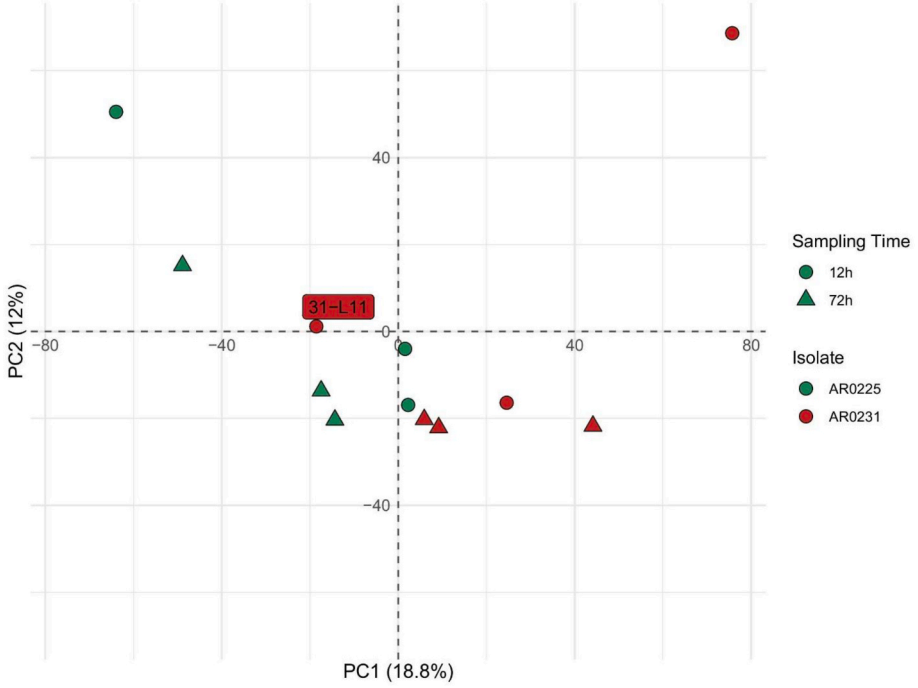

Fig. 2. Principal Component Analysis (PCA) of gene expression profiles in *A. rabiei* isolates AR0225 (low pathogenic) or AR0231 (highly pathogenic).

Table 1
DEGs involved in host interaction and immune evasion of *A. rabiei* isolates AR0231 (highly pathogenic) and AR0225 (lowly pathogenic) during infection of mature chickpea cv. PBA HatTrick

Gene symbol	Log_2FC[a]	Effector Score	Putative function	InterPro domain function
EKO05_0002468	8.12	0.45	Effector match: CoNIS1/MoNIS1/ChNIS1; Effector score: 0.45; contribute to host penetration, support nutrient uptake (Irieda et al., 2019; Nie et al., 2022)	Hypothetical protein
EKO05_0000089	6.04	−1.98	Effector match: FGL1/RsAGLIP1, contributes to the fungal pathogen's virulence by enhancing its ability to manage oxidative stress within host tissues, thereby promoting sustained infection and colonization (Li et al., 2019; Niu et al., 2013; Salomon et al., 2012)	Oxidoreductase
EKO05_0003549	5.39	0.58	Putative effector	Uncharacterized protein
EKO05_0010552	5.35	0.96	Effector match: PsGIP2/PsGIP1, inhibits host enzymes that target fungal cell walls (Damasceno et al., 2008; Mazumdar et al., 2021)	Glucanase inhibitor protein
EKO05_0010011	5.33	0.92	Putative effector	Uncharacterized protein
EKO05_0003368	2.35	−0.76	2-Aminomuconic semialdehyde dehydrogenase aids in the fungal pathogen's ability to adapt to and persist within the hostile environment (Gawel, 2024)	ALDH
EKO05_0001368	2.01	0.28	Effector match: PesCDA/VdPDA1/VnaChtBP (Volk et al., 2019; Zhang et al., 2022)	Chitin deacetylase
EKO05_0006947	−2.12	−0.34	Effector match: RsLysM/MoCDIP11, binds chitin to mask fungal presence (Jonge and Thomma, 2009; Kombrink et al., 2016; Kombrink and Thomma, 2013; Sanchez-Vallet et al., 2020)	LysM domain associated with immune evasion
EKO05_0006932	−3.55	0.41	Effector match: FolSix3 (Jangir et al., 2021)	Avr protein characteristics

[a] Positive Log_2FC values indicate upregulation in the highly pathogenic isolate AR0231, while negative values indicate downregulation in AR0231 compared to AR0225.

3.2.2. Nutrient uptake and regulatory roles

Genes associated with nutrient uptake and regulatory mechanisms were found to be differentially expressed between the isolates AR0231 and AR0225. EKO05_0000497 exhibited upregulation in AR0231 ($Log_2FC = 5.89$). This gene encodes a hexokinase enzyme, which plays a key role in carbohydrate metabolism and energy production (Table 2). Similarly, EKO05_0005154 ($Log_2FC = 4.40$) encoding a fructose-bisphosphate aldolase was also upregulated in AR0231, functioning as a key glycolytic enzyme facilitating energy production. Another upregulated gene in AR0231, EKO05_0002828 ($Log_2FC = 2.75$) was identified as a nicotinamide adenine dinucleotide (NAD) transporter. NAD supports mitochondrial redox balance and energy metabolism in the pathogen during host infection.

In contrast, several genes were downregulated in AR0231 that highlight differential regulation of nutrient acquisition and metabolic processes. EKO05_0008482 (Log2FC = −3.98), which encodes a KRR1 interacting zinc finger protein, is likely involved in regulatory processes linked to pathogenicity. EKO05_0002053 ($Log_2FC = -3.80$) encodes for a major facilitator superfamily (MFS) sugar transporter. Other

Table 2
DEGs involved in nutrient uptake and regulatory roles of *A. rabiei* isolates AR0231 (high) and AR0225 (low) pathogenic during infection on mature chickpea cv. PBA HatTrick

Gene ID	Log_2FC[a]	Putative function	InterPro domain function
EKO05_0000497	5.89	Supports energy production through carbohydrate metabolism	Hexokinase
EKO05_0005154	4.40	Fructose-bisphosphate aldolase, key enzyme in glycolysis	Glycolysis enzyme
EKO05_0002828	2.75	NAD transporter, facilitates energy production in mitochondria	NAD/FAD transporter
EKO05_0008482	−3.98	KRR1 interacting protein 1, likely involved in regulation	Zinc finger
EKO05_0002053	−3.80	MFS sugar transporter, involved in nutrient uptake from the host	MFS transporter
EKO05_0009280	−3.78	DNA Polymerase Delta Subunit 4 domain crucial for fungal growth and development (Baranovskiy et al., 2012; Jain et al., 2014; Prindle and Loeb, 2012)	DNA Polymerase Delta Subunit 4
EKO05_0000250	−2.71	Cytochrome P450 is involved in detoxification, metabolic adaptation, and sometimes oxidative stress management. CYPs can also considered as a housekeeping role in fungi (W. Chen et al., 2014; Črešnar and Petri, 2011; Park et al., 2008; Shin et al., 2018)	Cytochrome P450

[a] Positive Log_2FC values indicate upregulation in the highly pathogenic isolate AR0231, while negative values indicate downregulation in AR0231 compared to AR0225.

downregulated genes included EKO05_0009280 ($Log_2FC = -3.78$) encoding DNA Polymerase Delta Subunit 4 with a domain critical for fungal growth and development. Additionally, EKO05_0000250 ($Log_2FC = -2.71$) encoded a cytochrome P450 enzyme, involved in detoxification and metabolic adaptation (Table 2).

3.2.3. Validation of differential gene expression by qRT-PCR

To validate the trends seen in the transcriptomic findings, qRT-PCR analysis was performed on a subset of DEGs (FGL1, GIP1, PDA1, and Six 3) using cDNA from the same RNA samples from the transcriptome sequencing experiment as template. The results showed that four genes were significantly upregulated in the highly pathogenic *A. rabiei* isolate AR0231 compared to the less pathogenic isolate AR0225 (Fig. 3).

Among them, FGL1 and GIP1 exhibited the highest fold change expression, with mean values of 11.00 and 8.75, respectively. The gene PDA1 was also significantly upregulated, showing fold changes of 3.39. In contrast, Six 3 was downregulated with fold changes of 0.48 in AR0231 relative to AR0225.

4. Discussion

4.1. Effector molecules and immune evasion mechanisms

In *A. rabiei*, a range of candidate effector molecules were identified and found to be involved in suppressing host immune responses, enabling successful infection in chickpea. The differential expression of these candidate genes between isolates of varying pathogenicity (AR0225 and AR0231) reveals key insights into the molecular mechanisms underlying these processes. Effector prediction in *A. rabiei* has previously been conducted by the CCDM group using earlier genome annotations, and the present analysis builds on this by applying updated prediction methods to identify both known and novel candidates.

The EKO05_0002468 gene exhibited the highest upregulation in AR0231 ($Log_2FC = 8.12$). It matched with known effectors CoNIS1/MoNIS1/ChNIS1, which interfere with plant immune kinases such as BAK1 to suppress PAMP-triggered immunity (PTI) (Irieda et al., 2019; Nie et al., 2022). Another significantly upregulated gene, EKO05_0000089 (FGL1/RsAGLIP1), contributes to virulence by enabling the pathogen to manage oxidative stress within host tissues, supporting immune evasion. In *Fusarium graminearum*, the secreted lipase FGL1 is a virulence factor essential for infection of cereals, facilitating tissue colonization and lipid degradation (Niu et al., 2013; Salomon et al., 2012). Similarly, in *Rhizoctonia solani*, the effector AGLIP1 plays a significant role in pathogen virulence by inhibiting basal defenses and promoting disease development in plants (Li et al., 2019). The upregulation of EKO05_0000089 in *A. rabiei* reflects a conserved role in oxidative stress tolerance and virulence, supporting its function in immune evasion and pathogenicity. Gene EKO05_0010552 ($Log_2FC = 5.35$) matched with known effector PsGIP2/PsGIP1 encodes a glucanase inhibitor protein that suppresses host endo-β-1,3-glucanases targeting fungal cell walls. Glucanase inhibitor proteins (GIPs), such as PsGIP1 and PsGIP2 of *Phytophthora infestans* are secreted by the pathogen to inhibit host endo-β-1,3-glucanases, which are enzymes involved in the degradation of fungal cell walls. By inhibiting these host enzymes, GIPs help the pathogen evade the plant's immune responses, again facilitating infection and disease progression (Damasceno et al., 2008; Mazumdar et al., 2021). By producing higher levels of this inhibitor, the more pathogenic isolate likely maintains the integrity of its cell walls by suppressing host-derived glucanase activity. This suppression prevents enzymatic degradation, allowing the pathogen to resist host defenses and establish infection. EKO05_0001368, encoding a chitin-binding protein and matched with effector molecules PesCDA/VdPDA1/VnaChtBP, was upregulated in AR0231 ($Log_2FC = 2.01$) which play a critical role in fungal virulence by modifying chitin, a major component of fungal cell walls, to evade host immune recognition. In *V. dahliae* and *Fusarium* species, polysaccharide deacetylase (PDA1) deacetylates chitin into chitosan, a structural alteration that reduces recognition by plant chitin receptors, thereby suppressing chitin-triggered immunity and enhancing fungal survival within host tissues (Volk et al., 2019; Zhang et al., 2022). Similarly, in *A. rabiei,* this protein facilitates immune evasion through cell wall modification, through chitin deacetylase activity that converted chitin to chitosan, which is less recognizable by plant chitin receptors (Rafiei et al., 2021). Meanwhile, EKO05_0003368, encoding 2-aminomuconic semialdehyde dehydrogenase ($Log_2FC = 2.35$), was upregulated in *A. rabiei*, supporting its role in stress adaptation and metabolic regulation. In fungi, intermediates of the kynurenine pathway contribute to oxidative stress management, immune evasion, and virulence regulation (Gawel, 2024). The function of 2-aminomuconic semialdehyde dehydrogenase within this pathway is associated with detoxifying oxidative stress-related metabolites, facilitating

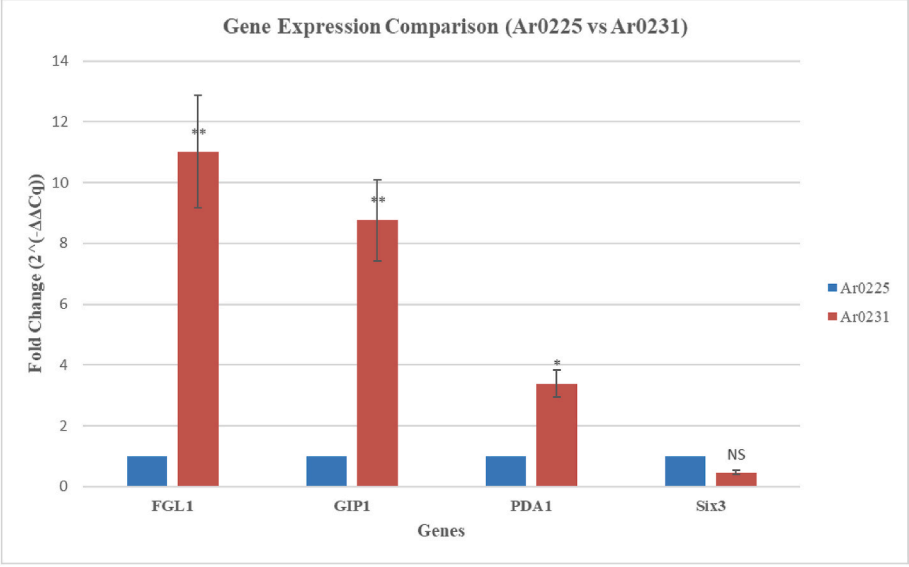

Fig. 3. Validation of differential gene expression by qRT-PCR. Expression levels were quantified using the 2^(-ΔΔCq) method, with EF1α and PEP1 as reference genes. Statistical significance was determined using the Kruskal–Wallis non-parametric test. Asterisks indicate significant differences ($p < 0.05$ = *, $p < 0.01$ = **, NS = Non-significant).

pathogen survival under the host's immune pressure (Gawel, 2024). This gene's upregulation in *A. rabiei* suggests a conserved role in fungal adaptation during host–pathogen interactions.

The gene EKO05_0003549 encodes a predicted serine-type endopeptidase, supported by InterProScan annotation (GO:0004252) and AlphaFold modelling. Secreted serine proteases are well-characterized virulence factors in many in fungal pathogens. In *Sclerotinia sclerotiorum*, subtilisin-like serine proteases are among the most highly upregulated genes during the early stages of host infection, suggesting a key role in pathogenicity (Seifbarghi et al., 2017). In contrast, EKO05_0010011 lacks characterized domains but is assigned to the ACW-9 (PTHR39602) protein family, a fungal-specific group of unknown function. Proteins with similar characteristics fungal-specific, secreted, and lacking conserved domains are commonly found in effector candidate sets (Sperschneider et al., 2016). Structural modelling (Supplementary Fig. 4) confirmed the presence of well-defined cores in both proteins, with extended N-terminal regions consistent with signal peptides, supporting both enzymatic activity in EKO05_0003549 and effector-like secretion features in EKO05_0010011.

In contrast, several genes were downregulated in AR0231, indicating shifts in the pathogen's strategy to prioritize mechanisms more directly aligned with enhanced pathogenicity. For example, gene EKO05_0006947, which is matched with effector molecule LysM/CDIP11 and containing the LysM domain, is known to mask fungal presence that aids in immune evasion by disrupting chitin-triggered immunity (Fig. 4). This was determined for RsLysM from *R. solani*, which binds with chitin and prevents fungal detection by the host's chitin receptors (Jonge and Thomma, 2009; Kombrink et al., 2016; Kombrink and Thomma, 2013; Sanchez-Vallet et al., 2020) and for MoCDIP11of *Magnaporthe oryzae*, identified as a cell death inducing protein (Guo et al., 2019; Li et al., 2020). The observed downregulation of the LysM domain-containing gene EKO05_0006947 in the highly pathogenic *A. rabiei* isolate AR0231 suggests a strategic shift from immune evasion toward rapid host colonization and tissue destruction. This aligns with the aggressive necrotrophic lifestyle, where the pathogen relies on inducing host cell death and efficiently acquiring nutrients rather than primarily focusing on evading the host's immune responses (Laluk and Mengiste, 2010; Oliver and Solomon, 2010). In contrast, gene like EKO05_0001368 (PesCDA/VdPDA1/VnaChtBP) involved in chitin deacetylation was upregulated in AR0231. Chitin deacetylases convert chitin into chitosan, a modification that helps pathogens evade host immune detection by reducing the release of chitin fragments that would otherwise trigger immune responses. This alternative strategy of chitin modification has been shown to enhance fungal virulence and colonization.

Of interest is the gene Six 3 (EKO05_0006932), which was downregulated in AR0231 ($Log_2FC = -3.55$). Six3 has a dual role in immune evasion and avirulence. In *Fusarium oxysporum*, FolSix3 functions as a virulence factor, inducing host cell death in *Nicotiana benthamiana*, but in *Solanum lycopersicum* (tomato), it acts as an avirulence (Avr 2) gene by triggering a resistance gene (R gene)-mediated immune response (Jangir et al., 2021). Importantly, Avr2 has also been shown to suppress pattern-triggered immunity, further highlighting its role in weakening basal host defenses (Tintor et al., 2020). This avirulence activity occurs through its interaction with the putative disease resistance protein RPP13-like 1 (LOC138339241) in tomato. While multiple homologous genes of RPP13-like proteins (XP_004499578.1, XP_004516528.1, XP_004512929.1, XP_027193384.1) are present in the chickpea genome, there is currently no experimental evidence demonstrating Six3 recognition by chickpea R proteins.

4.2. Nutrient acquisition and regulatory genes

Efficient nutrient acquisition and energy production are essential for fungal pathogenicity. In the highly pathogenic isolate AR0231, upregulation of glycolytic enzymes such as hexokinase (EKO05_0000497) and fructose-bisphosphate aldolase (EKO05_0005154) suggested increased metabolic activity during host colonization (Fleck and Brock, 2010; Laurian et al., 2019; Rui et al., 2007; Sambasivm et al., 2020). In addition, the upregulation of EKO05_0002828 in AR0231 is related to transport of essential cofactors like NAD, which is crucial for mitochondrial redox reactions and energy metabolism (Park et al., 2024;

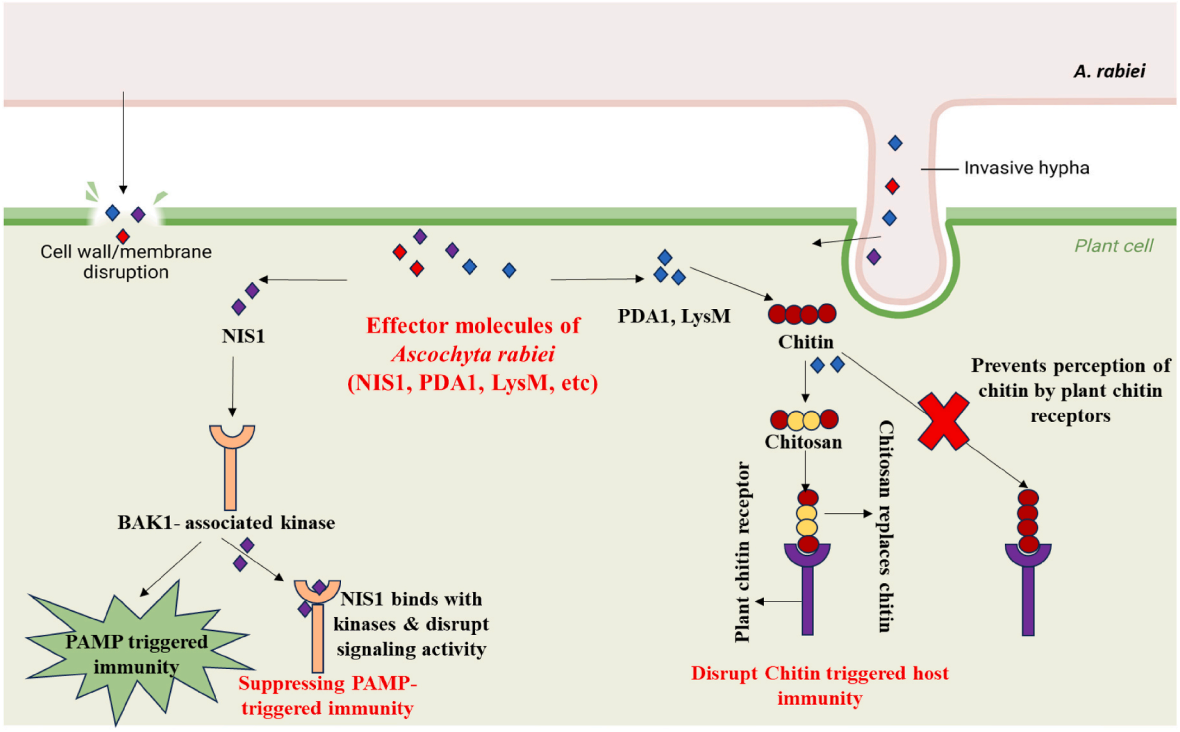

Fig. 4. A graphical representation of effector-mediated suppression of PAMP and chitin-triggered immunity by *A. rabiei* in chickpea host cells.

Xiao et al., 2018). Its upregulation likely supports increased mitochondrial energy production, enabling AR0231 to sustain higher metabolic activity during infection.

In contrast, genes involved in transcriptional regulation and nutrient transport, such as a zinc finger transcription factor (EKO05_0008482) and an MFS sugar transporter (EKO05_0002053), were downregulated in AR0231. This reflected a shift in infection strategy where the pathogen prioritized glycolytic energy production over controlled nutrient uptake (Schumacher et al., 2008; Sturm et al., 2017). Downregulation of other genes, such as cytochrome P450 (EKO05_0000250) and DNA polymerase delta subunit 4 (EKO05_0009280), further supported theory on reallocation of cellular resources toward aggressive colonization (W. Chen et al., 2014; Črešnar and Petri, 2011).

5. Conclusion

Through RNA sequencing, this study uncovered key molecular mechanisms underlying *A. rabiei* pathogenicity, focusing on differential gene expression related to immune evasion, nutrient acquisition, and metabolic adaptation. While many of these genes have homologs in other fungal pathogens, their expression and roles in *A. rabiei* pathogenicity have not been previously reported. The highly pathogenic isolate AR0231 showed significant upregulation of genes encoding known effector molecules and ones never described in *A. rabiei* before, along with energy production genes, emphasizing their roles in immune evasion and host tissue penetration and colonization. In contrast, several genes associated with glucose transport and cell signalling regulation such as zinc finger proteins and transcriptional regulators were downregulated in AR0231. This shift indicates a possible reallocation of metabolic resources away from general stress adaptation and toward specialized virulence strategies that promote aggressive infection. Such adaptations enable the highly pathogenic *A. rabiei* isolate to optimize resource allocation for successful host invasion and immunity suppression. These findings provide valuable insights into the molecular mechanisms of *A. rabiei* pathogenicity. Future research should focus on the functional and temporal validation of these candidate effectors.

CRediT authorship contribution statement

Mahmuda Binte Monsur: Writing – review & editing, Writing – original draft, Visualization, Validation, Software, Methodology, Investigation, Funding acquisition, Formal analysis. **Ido Bar:** Writing – review & editing, Supervision, Software, Resources, Funding acquisition, Data curation, Conceptualization. **Jonathan Wanderley Lawley:** Writing – review & editing, Software, Data curation. **Rebecca Ford:** Writing – review & editing, Supervision, Resources, Project administration, Funding acquisition, Data curation, Conceptualization.

Funding information

This research was funded by the Australian Grains Research and Development Corporation (GRDC) grant GRI2007-001RTX and Griffith University International Postgraduate Research Scholarship.

Declaration of competing interest

The authors declare that there are no conflicts of interest

Appendix A. Supplementary data

Supplementary data to this article can be found online at https://doi.org/10.1016/j.funbio.2025.101668.

References

Afgan, E., Baker, D., Batut, B., Van Den Beek, M., Bouvier, D., Ech, M., Chilton, J., Clements, D., Coraor, N., Grüning, B.A., Guerler, A., Hillman-Jackson, J., Hiltemann, S., Jalili, V., Rasche, H., Soranzo, N., Goecks, J., Taylor, J., Nekrutenko, A., Blankenberg, D., 2018. The galaxy platform for accessible, reproducible and collaborative biomedical analyses: 2018 update. Nucleic Acids Res. 46, W537–W544. https://doi.org/10.1093/nar/gky379.

Bar, I., Sambasivam, P.T., Davidson, J., Lee, R.C., Hobson, K., Ford, R., 2021. Current population structure and pathogenicity patterns of *Ascochyta rabiei* in Australia. Microb. Genomics 7. https://doi.org/10.1099/mgen.0.000627.

Baranovskiy, A.G., Lada, A.G., Siebler, H.M., Zhang, Y., Pavlov, Y.I., Tahirov, T.H., 2012. DNA polymerase and switch by sharing accessory subunits of DNA polymerase. J. Biol. Chem. 287, 17281–17287. https://doi.org/10.1074/jbc.M112.351122.

Basandrai, A.K., Basandrai, D., Pande, S., Sharma, M., Thakur, S.K., Thakur, H.L., 2007. Development of Ascochyta Blight (*Ascochyta rabiei*) in Chickpea as Affected by Host Resistance and Plant Age, pp. 77–78. https://doi.org/10.1007/s10658-007-9123-y.

Bretag, T.W., MacLeod, W.J., Kimber, R.B.E., Moore, K.J., Knights, E.J.C., Davidson, J.A., 2008. Management of ascochyta blight in chickpeas in Australia. Australas. Plant Pathol. 37, 486–497. https://doi.org/10.1071/AP08046.

Brown, N.A., Kosack, K.E.H., 2015. Secreted biomolecules in fungal plant pathogenesis. Fung. Biomol. 263–310.

Che, J., Shi, J., Lu, Y., Liu, Y., 2016. Validation of reference genes for normalization of gene expression by qRT - PCR in a resveratrol - producing entophytic fungus (*Alternaria* sp . MG1). AMB Express. https://doi.org/10.1186/s13568-016-0283-z.

Chen, S., Zhou, Y., Chen, Y., Gu, J., 2018. Fastp: an ultra-fast all-in-one FASTQ preprocessor. Bioinformatics 34, i884–i890. https://doi.org/10.1093/bioinformatics/bty560.

Chen, W., Lee, M.-K., Jefcoate, C., Kim, Sun-Chang, Chen, F., Yu, J.-H., 2014. Fungal Cytochrome P450 Monooxygenases : Their Distribution, Structure, Functions, Family Expansion, and Evolutionary Origin, 6, pp. 1620–1634. https://doi.org/10.1093/gbe/evu132.

Chen, Y., Lun, A.T.L., Smyth, G.K., 2014. Statistical analysis of next generation sequencing data. Stat. Anal. Next Gener. Seq. Data. https://doi.org/10.1007/978-3-319-07212-8.

Chongo, G., Gossen, B.D., Chongo, G., Gossen, B.D., 2001. Effect of plant age on resistance to Ascochyta rabiei in chickpea effect of plant age on resistance to *Ascochyta rabiei* in chickpea 0661. https://doi.org/10.1080/07060660109506956.

Christie, M., Sambasivam, P.T., Bar, I., 2021. Chickpea inoculation with *A . Rabiei* for ascochyta blight disease assessment under controlled conditions V . 2 inoculum preparation sowing. Protocol 2–5.

Črešnar, B., Petri, Š., 2011. Biochimica Et Biophysica Acta Cytochrome P450 Enzymes in the Fungal Kingdom, 1814, pp. 29–35. https://doi.org/10.1016/j.bbapap.2010.06.020.

Damasceno, C.M.B., Bishop, J.G., Ripoll, D.R., Win, J., Kamoun, S., Rose, J.K.C., 2008. Structure of the Glucanase Inhibitor Protein (GIP) Family from Phytophthora Species Suggests Coevolution with Plant Endo- B -1 , 3-Glucanases 21, pp. 820–830.

Debler, J.W., Lee, R.C., Singh, K.B., Kamphuis, L.G., Henares, B.M., 2025. Boscalid – a New Selectable Marker for *Ascochyta lentis* and *Ascochyta rabiei*, 129.

Ewels, P., Magnusson, M., Lundin, S., Käller, M., 2016. MultiQC: summarize analysis results for multiple tools and samples in a single report. Bioinformatics 32, 3047–3048. https://doi.org/10.1093/bioinformatics/btw354.

Flatschacher, D., Speckbacher, V., Zeilinger, S., 2022. qRAT : an R - based stand - alone application for relative expression analysis of RT - qPCR data. BMC Bioinf. 1–13. https://doi.org/10.1186/s12859-022-04823-7.

Fleck, C.B., Brock, M., 2010. Aspergillus fumigatus Catalytic Glucokinase and Hexokinase : Expression Analysis and Importance for Germination, 9, pp. 1120–1135. https://doi.org/10.1128/EC.00362-09.

Fondevilla, S., Krezdorn, N., Rotter, B., Kahl, G., Winter, P., 2015. *In planta* Identification of Putative Pathogenicity Factors from the Chickpea Pathogen *Ascochyta rabiei* by *De novo* Transcriptome Sequencing Using RNA-S. Front. Microbiol. 6, 1329. https://doi.org/10.3389/fmicb.2015.01329.

Foresto, E., Carezzano, M.E., Giordano, W., Bogino, P., 2023. Ascochyta blight in chickpea: an update. J. Fungi 9, 1–15. https://doi.org/10.3390/jof9020203.

Gawel, K., 2024. A Review on the Role and Function of Cinnabarinic Acid, a "Forgotten" Metabolite of the Kynurenine Pathway. Cells 13 (5), 453.

Guo, X., Zhong, D., Xie, W., He, Y., Zheng, Y., Lin, Y., Chen, Z., Han, Y., Tian, D., Liu, W., Wang, F., Wang, Z., Chen, S., 2019. Functional Identification of Novel Cell death-inducing Effector Proteins from *Magnaporthe Oryzae*.

Irieda, H., Inoue, Y., Mori, M., Yamada, K., Oshikawa, Y., Saitoh, H., Uemura, A., 2019. Conserved Fungal Effector Suppresses PAMP-triggered Immunity by Targeting Plant Immune Kinases, 116. https://doi.org/10.1073/pnas.1807297116.

Jain, R., Rajashankar, K.R., Buku, A., Johnson, R.E., Prakash, L., Prakash, S., Aggarwal, A.K., 2014. Crystal Structure of Yeast DNA Polymerase E Catalytic Domain, 9. https://doi.org/10.1371/journal.pone.0094835.

Jangir, P., Mehra, N., Sharma, K., Singh, N., Rani, M., 2021. Secreted in Xylem genes : drivers of host adaptation in *Fusarium oxysporum*. Front. Plant Sci. 12, 1–17. https://doi.org/10.3389/fpls.2021.628611.

Jones, D.A.B., Rybak, K., Bertazzoni, S., Tan, K.-C., Phan, H.T.T., Hane, J.K., 2021. Pathogenicity Effector Candidates and Accessory Genome Revealed by pan-genomic Analysis of *Parastagonospora nodorum*.

Jonge, R. De, Esse, H.P. Van, Kombrink, A., Shinya, T., Desaki, Y., Bours, R., Krol, S. Van Der, Shibuya, N., Joosten, M.H.A.J., Thomma, B.P.H.J., 2010. Conserved fungal LysM EffectorEcp6 prevents chitin-triggered immunity in plants. Science 329, 953–956.

Jonge, R. De, Thomma, B.P.H.J., 2009. Fungal Lysm Effectors : Extinguishers of Host Immunity ?, pp. 151–157. https://doi.org/10.1016/j.tim.2009.01.002.
Kombrink, A., Rovenich, H., Shi-Kunne, X., Thomma, B.P.H.J., 2016. *Verticillium dahliae* LysM effectors differentially contribute to virulence on plant hosts. Mol. Plant Pathol. 8, 596–608. https://doi.org/10.1111/mpp.12520.
Kombrink, A., Thomma, B.P.H.J., 2013. Lysm Effectors : Secreted Proteins Supporting Fungal Life, 9. https://doi.org/10.1371/journal.-ppat.1003769.
Kruskal, W.H., Wallis, W.A., 1952. Use of ranks in one-criterion variance analysis. J. Am. Stat. Assoc. 47, 259–272.
Laluk, K., Mengiste, T., 2010. Necrotroph attacks on plants : wanton destruction or covert extortion. Arab. B. 8, 1–34.
Laurian, R., Dementhon, K., Doumèche, B., Soulard, A., Noel, T., Lemaire, M., Cotton, P., 2019. Hexokinase and Glucokinases are Essential for Fitness and Virulence in the Pathogenic Yeast Candida albicans Strains and Growth Conditions, 10, pp. 1–18. https://doi.org/10.3389/fmicb.2019.00327.
Li, L., Zhu, X., Zhang, Y., Cai, Y., Wang, Jing-yi, Liu, M., Wang, Jiao-yu, Bao, J., Lin, F., 2022. Research on the molecular interaction mechanism between plants and pathogenic fungi. Int. J. Mol. 23 (9), 4658.
Li, S., Peng, X., Wang, Y., Hua, K., Xing, F., Zheng, Y., 2019. The Effector AGLIP1 in Rhizoctonia solani AG1 IA Triggers Cell Death in Plants and Promotes Disease Development Through Inhibiting PAMP-triggered Immunity in *Arabidopsis thaliana*, 10, pp. 1–12. https://doi.org/10.3389/fmicb.2019.02228.
Li, Y., Han, Y., Qu, M., Chen, J., Chen, X., Geng, X., Tyler, B.M., 2020. Apoplastic cell death-inducing proteins of filamentous plant pathogens : roles in plant-pathogen interactions. Front. Genet. 11. https://doi.org/10.3389/fgene.2020.00661.
Liao, Y., Smyth, G.K., Shi, W., 2013. Sequence analysis featureCounts : an efficient general purpose program for assigning sequence reads to genomic features 1–8. https://doi.org/10.1093/bioinformatics/btt656.
Mazumdar, P., Singh, P., Kethiravan, D., Ramathani, I., 2021. Late blight in tomato : insights into the pathogenesis of the aggressive pathogen *Phytophthora infestans* and future research priorities. Planta 253, 1–24. https://doi.org/10.1007/s00425-021-03636-x.
Nene, Y., Reddy, M., Haware, M., Ghanekar, A., Amin, K., 2012. Field Diagnosis of Chickpea Diseases and their Control.
Nene, Y.L., 2008. A review of ascochyta blight of chickpea A review of ascochyta blight of chickpea * 6147. https://doi.org/10.1080/09670878209370675.
Newman, T.E., Jacques, S., Grime, C., Kamphuis, F.L., Lee, R.C., Berger, J., Kamphuis, L. G., 2021. Identification of novel sources of resistance to ascochyta blight in a collection of wild cicer accessions. Phytopathology 111, 369–379. https://doi.org/10.1094/PHYTO-04-20-0137-R.
Nie, J., Zhou, W., Lin, Y., Liu, Z., Yin, Z., Huang, L., 2022. Two NIS1-like proteins from apple canker pathogen (Valsa Mali) play distinct roles. In: Plant Recognition and Pathogen Virulence.
Niu, X., Zheng, Z., Feng, Y., Guo, W., Wang, X., 2013. The Fusarium Graminearum virulence factor FGL targets an FKBP12 immunophilin of wheat. Gene 525, 77–83. https://doi.org/10.1016/j.gene.2013.04.052.
Okonechnikov, K., Conesa, A., García-Alcalde, F., 2016. Qualimap 2: advanced multi-sample quality control for high-throughput sequencing data. Bioinformatics 32, 292–294. https://doi.org/10.1093/bioinformatics/btv566.
Oliver, R.P., Solomon, P.S., 2010. New developments in pathogenicity and virulence of necrotrophs. Curr. Opin. Plant Biol. 13, 415–419. https://doi.org/10.1016/j.pbi.2010.05.003.
Pande, S., Siddique, K.H.M., Kishore, G.K., Bayaa, B., Gaur, P.M., Gowda, C.L.L., Bretag, T.W., Crouch, J.H., 2005. Ascochyta blight of chickpea (*Cicer arietinum* L .): a review of biology , pathogenicity , and disease management. Aust. J. ofAgricultural Res. 317–332.
Park, J., Lee, N., Kim, H., Kim, D., Shin, S., Choi, S., Ja, G., Son, H., 2024. A mitochondrial NAD/NADH kinase governs fungal virulence through an oxidative stress response and arginine biosynthesis in *Fusarium graminearum*. Microbiol. Res. 283, 127692. https://doi.org/10.1016/j.micres.2024.127692.
Park, Jongsun, Lee, S., Choi, J., Ahn, K., Park, B., Park, Jaejin, Kang, S., Lee, Y., 2008. Fungal Cytochrome P450 Database, 11, pp. 1–11. https://doi.org/10.1186/1471-2164-9-402.
Pfaffl, M.W., 2001. A new mathematical model for relative quantification in real-time RT – PCR. Nucleic Acids Res. 29, 16–21.
Prindle, M.J., Loeb, L.A., 2012. DNA Polymerase Delta in DNA Replication and Genome Maintenance, 682, pp. 666–682. https://doi.org/10.1002/em.
Qi, J., Asl, H.F., Björkegren, J., Michoel, T., 2014. Krux: Matrix-Based Non-parametric Eqtl Discovery, pp. 1–7.
Rafiei, V., Vélëz, H., Tzelepis, G., 2021. The role of glycoside hydrolases in phytopathogenic fungi and oomycetes virulence. Int. J. Mol. Sci. 22. https://doi.org/10.3390/ijms22179359.
Rui, O., Hahn, M., Hahn, M., 2007. The Botrytis cinerea hexokinase , Hxk1 , but not the glucokinase , Glk1 , is required for normal growth and sugar metabolism , and for pathogenicity on fruits 2791–2802. https://doi.org/10.1099/mic.0.2007/006338-0.
Salomon, S., Gácser, A., Frerichmann, S., Kröger, C., Schäfer, W., Voigt, C.A., 2012. The Secreted Lipase FGL1 is Sufficient to Restore the Initial Infection Step to the Apathogenic *Fusarium graminearum* MAP Kinase Disruption Mutant Δgpmk1, pp. 23–37. https://doi.org/10.1007/s10658-012-0017-2.
Sambasivam, P., Mehmood, Y., Bar, I., Davidson, J., Hobson, K., Moore, K., Ford, R., 2020a. Evidence of recent increased pathogenicity within the Australian *Ascochyta rabiei* population. bioRixv 1–35.
Sambasivam, P., Mehmood, Y., Bar, I., Davidson, J., Hobson, K., Moore, K., Ford, R., 2020b. Evidence of recent increased pathogenicity within the Australian *Ascochyta rabiei* population. bioRxiv 21, 1–9.
Sambasivm, P., Mehmood, Y., Bar, I., Davidson, J., Hobson, K., Moore, K., Ford, R., 2020. Evidence of recent increased pathogenicity within the Australian *Ascochyta rabiei* population 1–35. https://doi.org/10.1101/2020.06.28.175653.
Sanchez-Vallet, A., Tian, H., Rodriguez-Moreno, L., Valkenburg, J., Id, R.S., Wawra, S., Kombrink, A., 2020. A secreted LysM effector protects fungal hyphae through chitin-dependent homodimer polymerization. PLoS Pathog. 1–21. https://doi.org/10.1371/journal.ppat.1008652.
Schumacher, J., Larrinoa, I.F. De, Tudzynski, B., 2008. Calcineurin-responsive zinc finger transcription factor CRZ1 of *Botrytis cinerea* is required for growth. Develop. Full Virulence Bean Plant 7, 584–601. https://doi.org/10.1128/EC.00426-07.
Seifbarghi, S., Borhan, M.H., Wei, Y., Coutu, C., Robinson, S.J., Hegedus, D.D., 2017. Changes in the *Sclerotinia sclerotiorum* transcriptome during infection of *Brassica napus* 1–37. https://doi.org/10.1186/s12864-017-3642-5.
Shah, R.M., Williams, A.H., Hane, J.K., Lawrence, J.A., Farfan-Caceres, L.M., Debler, J. W., Oliver, R.P., Lee, R.C., 2020. Reference genome assembly for Australian *Ascochyta rabiei* isolate ArME14. G3 Gene Genom. Genet. 10, 2131–2140. https://doi.org/10.1534/g3.120.401265.
Sharma, M., Ghosh, R., 2016. An update on genetic resistance of chickpea to ascochyta blight. Agronomy 8. https://doi.org/10.3390/agronomy6010018.
Sharma, M., Pande, S., 2010. Effect of Growth Stages of Chickpea on the Genetic Resistance of Ascochyta Blight, pp. 325–331. https://doi.org/10.1007/s10658-010-9641-x.
Shin, J., Kim, J., Lee, Y., Son, H., 2018. Fungal Cytochrome P450s and the P450 Complement (Cypome) of Fusarium graminearum, pp. 76–91. https://doi.org/10.3390/toxins10030112.
Singh, K.B., Reddy, M.V., 1993. Resistance to Six Races of *Ascochyta rabiei* in the World Germplasm Collection of Chickpea, 189, pp. 186–189. https://doi.org/10.2135/cropsci1993.0011183X003300010033x.
Singh, R., Kumar, K., Purayannur, S., Chen, W., Verma, P.K., 2022. *Ascochyta rabiei* : a threat to global chickpea production. Mol. Plant Pathol. 1241–1261. https://doi.org/10.1111/mpp.13235.
Singh, S. kumar, Shree, A., Verma, S., Singh, K., Shree, A., Singh, R., 2023. The nuclear effector ArPEC25 from the necrotrophic fungus *Ascochyta rabiei* targets the chickpea transcription factor ca β LIM1a and negatively modulates lignin biosynthesis, increasing host susceptibility. Plant Cell. https://doi.org/10.1101/2021.09.02.458738.
Sperschneider, J., Gardiner, D.M., Dodds, P.N., Tini, F., Covarelli, L., Singh, K.B., Manners, J.M., Taylor, J.M., 2016. Methods effector P: Predicting Fungal Effector Proteins from Secretomes Using Machine Learning, pp. 743–761.
Sturm, M., Cheng, J., Baßler, J., Beckmann, R., Hurt, E., 2017. Interdependent action of KH domain proteins Krr1 and Dim 2 drive the 40S platform assembly. Nat. Commun. 8. https://doi.org/10.1038/s41467-017-02199-4.
Tintor, N., Paauw, M., Rep, M., Takken, F.L.W., 2020. The root-invading pathogen *Fusarium oxysporum* targets pattern-triggered immunity using both cytoplasmic and apoplastic effectors. Mol. Plant Pathol. 1479–1492. https://doi.org/10.1111/nph.16618.
Trapero-Casas, A., Kaiser, W.J., 1992. Development of *Didymella rabiei*, the teleomorph of *Ascochyta rabiei*, on chickpea straw. Phytopathology 82, 1261–1266.
Vaghefi, N., Bar, I., Lawley, J.W., Sambasivam, P., Christie, M., Ford, R., 2024. Population-level whole genome sequencing of *Ascochyta rabiei* identifies genomic loci associated with isolate aggressiveness. Microbial Genomics. 10 (11), 001326.
Vasimuddin, M., Misra, S., Li, H., Aluru, S., 2019. Efficient architecture-aware acceleration of BWA-MEM for multicore systems. In: Proc. - 2019 IEEE 33rd Int. Parallel Distrib. Process. Symp. IPDPS 2019, pp. 314–324. https://doi.org/10.1109/IPDPS.2019.00041.
Verma, S., Gazara, R.K., Verma, P.K., 2017. Transcription factor repertoire of necrotrophic fungal phytopathogen *Ascochyta rabiei*: predominance of MYB transcription factors as potential regulators of secretome. Front. Plant Sci. 8, 1037. https://doi.org/10.3389/fpls.2017.01037.
Volk, H., Marton, K., Flaj, M., 2019. Chitin-binding protein of *Verticillium nonalfalfae* disguises fungus from plant chitinases and suppresses chitin-triggered host immunity. Mol. Plant Microbe Interact. 32, 1378–1390. https://doi.org/10.1094/MPMI-03-19-0079-R.
Wickham, H., 2009. ggplot 2: Elegant Graphics for Data Analysis. springer, New York. https://doi.org/10.18637/jss.v077.b02.
Xiao, W., Wang, R., Handy, D.E., Loscalzo, J., 2018. NAD(H) and NADP(H) redox couples and cellular. Energy Metabolism 28, 251–272. https://doi.org/10.1089/ars.2017.7216.
Zhang, S., Li, C., Si, J., Han, Z., Chen, D., 2022. Action mechanisms of effectors in plant-pathogen interaction. Int. J. Mol. 23 (12), 6758.